

# Characterization of the [2Fe-2S] Cluster of *Escherichia coli* Transcription Factor IscR

Angela S. Fleischhacker,<sup>†</sup> Audria Stubna,<sup>§</sup> Kuang-Lung Hsueh,<sup>‡</sup> Yisong Guo,<sup>§</sup> Sarah J. Teter,<sup>†</sup> Justin C. Rose,<sup>†</sup> Thomas C. Brunold,<sup>||</sup> John L. Markley,<sup>‡</sup> Eckard Münck,<sup>§</sup> and Patricia J. Kiley<sup>\*,†</sup>

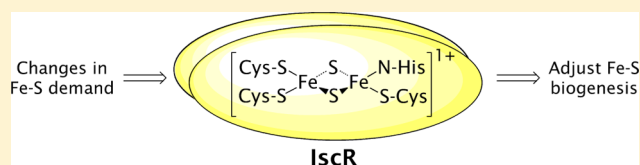
<sup>†</sup>Department of Biomolecular Chemistry, University of Wisconsin, Madison, Wisconsin 53706, United States

<sup>‡</sup>Department of Biochemistry, University of Wisconsin, Madison, Wisconsin 53706, United States

<sup>§</sup>Department of Chemistry, Carnegie Mellon University, Pittsburgh, Pennsylvania 15213, United States

<sup>||</sup>Department of Chemistry, University of Wisconsin, Madison, Wisconsin 53706, United States

**ABSTRACT:** IscR is an Fe–S cluster-containing transcription factor involved in a homeostatic mechanism that controls Fe–S cluster biogenesis in *Escherichia coli*. Although IscR has been proposed to act as a sensor of the cellular demands for Fe–S cluster biogenesis, the mechanism by which IscR performs this function is not known. In this study, we investigated the biochemical properties of the Fe–S cluster of IscR to gain insight into the proposed sensing activity. Mössbauer studies revealed that IscR contains predominantly a reduced [2Fe-2S]<sup>+</sup> cluster in vivo. However, upon anaerobic isolation of IscR, some clusters became oxidized to the [2Fe-2S]<sup>2+</sup> form. Cluster oxidation did not, however, alter the affinity of IscR for its binding site within the *iscR* promoter in vitro, indicating that the cluster oxidation state is not important for regulation of DNA binding. Furthermore, characterization of anaerobically isolated IscR using resonance Raman, Mössbauer, and nuclear magnetic resonance spectroscopies leads to the proposal that the [2Fe-2S] cluster does not have full cysteinyl ligation. Mutagenesis studies indicate that, in addition to the three previously identified cysteine residues (Cys92, Cys98, and Cys104), the highly conserved His107 residue is essential for cluster ligation. Thus, these data suggest that IscR binds the cluster with an atypical ligation scheme of three cysteines and one histidine, a feature that may be relevant to the proposed function of IscR as a sensor of cellular Fe–S cluster status.



*Escherichia coli* transcription factor IscR regulates the expression of more than 40 genes, including the *isc* operon encoding IscR itself and the Isc proteins responsible for Fe–S cluster biogenesis.<sup>1</sup> IscR, which was found to contain a [2Fe-2S] cluster upon anaerobic isolation, requires a functional Isc pathway to repress transcription of the *isc* operon,<sup>2</sup> suggesting an intimate link between the Fe–S cluster occupancy of IscR and its function as a repressor of the Isc pathway. The noted connection further led to the hypothesis that IscR acts as a sensor of the cellular demands for Fe–S cluster biogenesis.<sup>2,3</sup> Although the mechanism of sensing is unknown, atypical Fe–S cluster protein properties such as inefficient acquisition of the Fe–S cluster by IscR or unusual sensitivity to oxidants could make the Fe–S cluster occupancy of IscR sensitive to the general cellular demands for Fe–S cluster biogenesis. Characterization of the biochemical properties of the Fe–S cluster of IscR is an important first step toward the development of a detailed understanding of the sensing mechanism employed by IscR.

One fundamental question regarding the cluster-bound state of IscR involves the amino acid side chains required for cluster ligation. Most [2Fe-2S] clusters have all cysteinyl (Cys)<sub>4</sub> ligation. Notable exceptions are the Rieske proteins, which have [2Fe-2S] clusters featuring (Cys)<sub>2</sub>(His)<sub>2</sub> ligation. Cys92, Cys98, and Cys104 are the only cysteines in IscR, and all three have been shown by mutagenesis studies to be necessary for the

formation of the holoprotein.<sup>4,5</sup> Furthermore, both [2Fe-2S] and clusterless IscR were found to exist as homodimers in solution.<sup>5</sup> Therefore, if the cluster of IscR had full cysteinyl ligation typical of Fe–S clusters, the cluster would have to bridge the subunits of the dimer. Consistent with this model, anaerobically isolated IscR was ~50% occupied with cluster.<sup>5</sup> However, the EPR *g* values for *E. coli* [2Fe-2S]<sup>+</sup>-IscR of 1.99, 1.93, and 1.88<sup>2</sup> are inconsistent with all cysteinyl ligation of the Fe–S cluster. The *g* values of [2Fe-2S]<sup>+</sup> clusters are influenced by ligand coordination.<sup>6,7</sup> Importantly, the average *g* value (*g*<sub>av</sub>) of ~1.93 for [2Fe-2S]<sup>+</sup>-IscR is lower than values reported for proteins that ligate [2Fe-2S] clusters via four cysteines (*g*<sub>av</sub> ~ 1.97), suggesting that the IscR-bound cluster has an unusual ligation scheme.

IscR is a member of the Rrf2 family of transcription factors, predicted to contain a characteristic winged helix–turn–helix DNA-binding domain (PF02082<sup>8</sup>). The family members are not well characterized, but the presence of conserved cysteines in several of them suggests that a subset of these proteins may ligate Fe–S clusters. While previous studies have shown that IscR from *E. coli* contains a [2Fe-2S] cluster that can be

Received: March 6, 2012

Revised: May 11, 2012

Published: May 14, 2012



reversibly oxidized and reduced,<sup>2</sup> neither the type of cluster that is present in vivo nor its in vivo oxidation state has been examined. Such information is becoming increasingly important as differences in isolation methods have emerged as a factor affecting the type of isolated cluster because of the potential for cluster conversions. For example, recent studies of a related transcription factor in the Rrf2 family, the NO sensor NsrR, raised the question of whether the functional form of NsrR contains a [2Fe-2S] or a [4Fe-4S] cluster.<sup>9</sup>

In this study, cluster-bound IscR of *E. coli* was characterized in vivo and in vitro to further our understanding of the function of IscR as a sensor of the Fe-S cluster status of the cell. First, to determine the nature of the cluster bound to IscR in vivo, Mössbauer spectra of IscR in whole cells were recorded. A combination of resonance Raman, nuclear magnetic resonance (NMR), and Mössbauer spectroscopies were then used to characterize the Fe-S cluster of isolated IscR and to identify its ligands. In conjunction, mutagenesis studies were performed to explore possible ligation schemes. The effects of substituting IscR residues with alanine or other amino acids were analyzed in vitro by quantifying the Fe-S cluster occupancy of the anaerobically isolated IscR variants and in vivo by monitoring the ability of the IscR variants to repress the *iscR* promoter in a *lacZ* reporter strain. Finally, we examined the effect of the Fe-S cluster oxidation state on DNA binding by IscR using fluorescence polarization assays. The results led to the proposal that *E. coli* IscR has an unusual (Cys)<sub>3</sub>(His)<sub>1</sub> Fe-S cluster ligation scheme, which may be relevant to the ability of IscR to function as a sensor of the cellular Fe-S cluster status. A similar ligation scheme has recently been proposed for the Fra2-Grx3 heterodimeric complex, which is involved in iron regulation in yeast and has possible sensor functions.<sup>10,11</sup>

## METHODS

**Mössbauer Spectroscopic Analysis of Anaerobically Isolated IscR.** Wild-type IscR was isolated anaerobically from *E. coli* strain PK7901 (BL21Δ*crp*-*bs990*Δ*fnr* harboring pPK6161) as described previously,<sup>1</sup> except that cells were grown in Chelex-treated glucose M9 medium supplemented with 10 μM [<sup>57</sup>Fe]ferrous ethylenediammonium sulfate, and a Poly-CatA ion exchange column chromatography step was used in place of heparin ion exchange. A high-performance liquid chromatography (HPLC) Poly-CatA ion exchange column was equipped with a column chiller and attached to a Beckman HPLC system in an anaerobic chamber.<sup>12</sup> The sample was loaded and subsequently washed with 95 mL of 50 mM Tris buffer (pH 7.4) containing 0.1 M KCl, 10% glycerol, and 1 mM dithiothreitol. The protein was eluted with a 12 mL gradient (from 2 to 50%) of 50 mM Tris buffer (pH 7.4) containing 1.0 M KCl, 10% glycerol, and 1 mM dithiothreitol at a rate of 0.5 mL/min. The eluted protein was subsequently purified and concentrated over size exclusion and BioRex-70 columns, respectively, as described previously,<sup>1</sup> except that 50 mM Tris buffer (pH 7.4) was used in place of HEPES buffer. The protein was subsequently transferred to a Mössbauer sample cup, and spectra of the as-purified IscR sample were recorded. The sample then was thawed and exposed to air for 5 min, and spectra were recorded. Finally, the sample was thawed in an anaerobic chamber, and 10 μL of 35 mM dithionite was added. After being stirred for 30–60 s, the sample was rapidly frozen and analyzed by Mössbauer spectroscopy, as described previously.<sup>13</sup>

**Whole Cell Mössbauer Spectroscopy.** Cell cultures were grown and subsequently prepared for and analyzed by whole cell Mössbauer spectroscopy, as described previously<sup>14,15</sup> with minor modifications. Strain PK7901 overexpressing IscR or a strain lacking overexpressed IscR (BL21 + pET11a) was grown in the presence of 10 μM [<sup>57</sup>Fe]ferrous ethylenediammonium sulfate,<sup>12</sup> and the cell pellet was washed with 50 mM Tris buffer (pH 7.4) containing 0.1 M KCl and 10% glycerol before the sample was transferred to a Mössbauer sample cup and frozen on dry ice.

**Resonance Raman Spectroscopy.** Wild-type (WT) IscR was isolated from strain PK7901 as described for Mössbauer spectroscopy. Spectra were recorded upon excitation with an Ar<sup>+</sup> ion laser (Coherent I-305) with incident power in the 50–100 mW range. The scattered light was collected using an ~135° backscattering arrangement, dispersed by a triple monochromator (Acton Research, equipped with 300, 1200, and 2400 grooves/mm gratings) and analyzed with a deep depletion, back-thinned CCD camera (Princeton Instruments Spec X: 100BR). All spectra were recorded at 77 K on frozen protein samples contained in NMR tubes that were immersed in a liquid N<sub>2</sub>-filled EPR dewar to prevent photodegradation.

**Isolation of IscR for Visible Spectroscopy, NMR Spectroscopy, and Binding Assays.** IscR and IscR variants were isolated under anaerobic conditions using heparin ion exchange, gel filtration, and BioRex-70 column chromatographies.<sup>1</sup> The protein concentration (reported on a per-monomer basis) and iron content were determined colorimetrically.<sup>2</sup> Absorption spectra of IscR (isolated from strain PK8581) and IscR variants were recorded anaerobically in 10 mM HEPES buffer (pH 7.2) containing 0.2 M KCl in sealed cuvettes.<sup>12</sup>

**Strain Construction and β-Galactosidase Assays.** Chromosomally encoded mutants of *iscR* were constructed as described previously.<sup>5</sup> Three independent isolates of each strain were grown in MOPS minimal medium with 0.2% glucose under anaerobic conditions<sup>1</sup> to an OD<sub>600</sub> of ~0.1 and assayed for β-galactosidase activity.<sup>16</sup>

**Preparation of <sup>15</sup>N-Labeled Protein Samples.** WT IscR was isolated from strain PK8581 grown with <sup>15</sup>N-labeled NH<sub>4</sub>Cl (Cambridge Isotope Laboratories) and without the addition of casamino acids to generate a uniformly <sup>15</sup>N-labeled IscR sample [[U-<sup>15</sup>N]IscR(WT)]. A second sample was prepared from cells grown by the same protocol, except that 0.1 g/L unlabeled L-histidine was added during cell growth [[U-<sup>15</sup>N,NA-His]IscR(WT)]. A third sample uniformly labeled with <sup>15</sup>N was prepared from the IscR variant in which both His143 and His145 were substituted with Ala [[U-<sup>15</sup>N]IscR-(H143A/H145A)]. Following isolation and purification, these samples were concentrated under anaerobic conditions to 1.5 mM for NMR analysis.

**<sup>15</sup>N NMR Spectroscopy.** A 5-fold molar excess of sodium dithionite was added to reduce the samples. Protein samples were transferred to NMR tubes equipped with a J. Young valve (Wilma, Vineland, NJ) under anaerobic conditions and then sealed. <sup>15</sup>N NMR spectra were recorded on a Bruker 500 MHz NMR spectrometer. Short recycling delays were used to suppress signals from slowly relaxing nuclei distant from the cluster. The pH was measured before and after data collection and was found to be unchanged. Chemical shifts were referenced to sodium 2,2-dimethyl-2-silapentane-5-sulfonate (DSS). NMR data were collected at two temperatures (298

and 288 K) to identify hyperfine-shifted signals from their temperature dependence.

**DNA Binding Fluorescence Assays.** Binding of IscR to double-stranded DNA (dsDNA) containing the *iscR* binding site (positions −42 to −12 relative to the transcription start site) was assessed using fluorescence polarization assays as described previously.<sup>5</sup> The assays were performed under anaerobic conditions with and without added dithionite using wild-type IscR from strain PK8581 that was isolated under anaerobic conditions as described previously<sup>1</sup> but exposed to air for 5 min.

## RESULTS

**Mössbauer Studies of IscR as Purified and in Whole Cells.** The 4.2 K Mössbauer spectra show that IscR is a mixture of oxidized and reduced states upon anaerobic isolation (data not shown). Therefore, as-isolated IscR was exposed to air to obtain the spectrum of the oxidized state (Figure 1), and the

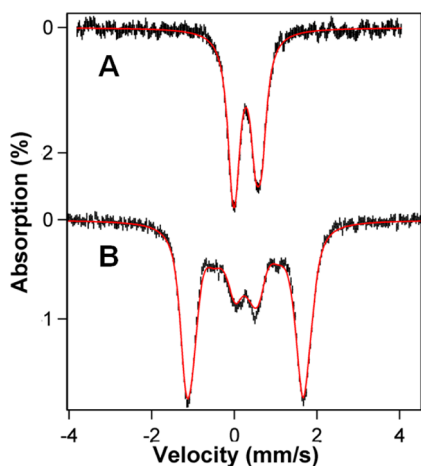


**Figure 1.** 4.2 K Mössbauer spectra of anaerobically isolated IscR that has been exposed to air recorded in zero field (A) and at  $B = 8.0$  T (B). Solid lines are simulations assuming an  $S = 0$  cluster using the nested set of parameters:  $\Delta E_Q(1) = -0.48$  mm/s,  $\delta(1) = 0.27$  mm/s, and  $\eta(1) = 0.5$ ;  $\Delta E_Q(2) = 0.72$  mm/s,  $\delta(2) = 0.30$  mm/s, and  $\eta(2) = 0.5$ .

sample was subsequently reduced with dithionite to obtain the spectrum of the reduced state (Figure 2). The 4.2 K spectrum of oxidized IscR exhibits two overlapping quadrupole doublets in a 1:1 intensity ratio with the following quadrupole splittings and isomer shifts:  $\Delta E_Q(1) = -0.48$  mm/s,  $\delta(1) = 0.27$  mm/s,  $\Delta E_Q(2) = 0.72$  mm/s, and  $\delta(2) = 0.30$  mm/s. These parameters are characteristic of  $[2\text{Fe-2S}]^{2+}$  clusters. In their 2+ oxidation state,  $[2\text{Fe-2S}]^{2+}$  clusters possess a diamagnetic ground state, and this expectation is confirmed by the 8.0 T data of IscR (Figure 1B); thus, the 8.0 T spectrum can be fit by assuming the absence of  $^{57}\text{Fe}$  magnetic hyperfine interactions. This spectrum also yields the asymmetry parameter (see below) of the electric field gradient (EFG) tensors [ $\eta(1) = \eta(2) = 0.5$ ]. The assignment of the four lines described above assumes two nested doublets in Figure 1A; however, a non-nested assignment [ $\Delta E_Q(1) = -0.57$  mm/s,  $\delta(1) = 0.23$  mm/s,  $\Delta E_Q(2) = 0.64$  mm/s, and  $\delta(2) = 0.34$  mm/s] fits both spectra as well as the nested set.

Figure 2 shows 4.2 K Mössbauer spectra of dithionite-reduced IscR recorded in parallel applied magnetic fields as indicated. These spectra have features typically observed for

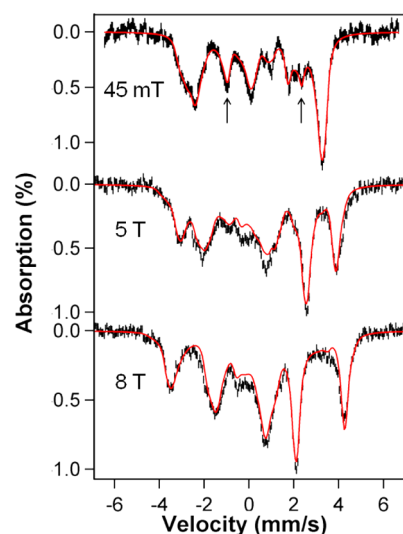


**Figure 2.** 4.2 K Mössbauer spectra of dithionite-reduced IscR recorded in a parallel applied field as indicated. The solid red lines are spectral simulations based on eq 1 using the parameters listed in Table 1. For the simulation of the 45 mT spectrum, we have added a doublet for a minor contaminant (8%, arrows) with the following values:  $\Delta E_Q = 3.35$  mm/s, and  $\delta = 0.70$  mm/s.

$[2\text{Fe-2S}]^+$  clusters, and accordingly, we have analyzed them with an  $S = 1/2$  spin Hamiltonian pertinent for the ground state of an antiferromagnetically coupled pair of high-spin  $\text{Fe}^{3+}$  ( $S = 5/2$ ) and  $\text{Fe}^{2+}$  ( $S = 2$ ) atoms, as described elsewhere.

$$\mathcal{H} = \beta \mathbf{S} \cdot \mathbf{g} \cdot \mathbf{B} + \sum_{i=1,2} \mathbf{S} \cdot \mathbf{A}_i \cdot \mathbf{I}_i - g_n \beta_n \mathbf{B} \cdot \mathbf{I}_i + \mathcal{H}_Q(i) \quad (1)$$

with

$$\mathcal{H}_Q = \frac{eQV_{zz}}{12} [3I_z^2 - 15/4 + \eta(I_x^2 - I_y^2)] \text{ and } \eta = (V_{xx} - V_{yy})/V_{zz}$$

In eq 1, all symbols have their conventional meanings.<sup>17</sup> The solid red lines in Figure 2 are spectral simulations using eq 1 with the parameters listed in Table 1. Because the  $\mathbf{g}$  tensor is rather isotropic, the orientation of the magnetic hyperfine tensors,  $\mathbf{A}_i$ , and the EFG tensors relative to  $\mathbf{g}$  cannot be determined from a powder spectrum; for the simulations, we have used  $\mathbf{g} = g_{\text{av}} = 1.93$  according to the published EPR data<sup>2</sup> of IscR.

**Table 1.** Mössbauer and EPR Parameters of Selected  $[2\text{Fe-2S}]^+$  Proteins

	IscR		<i>Aquifex aeolicus</i> Fd1 <sup>a</sup>	
	g values of 1.88, 1.93, 1.99		g values of 1.88, 1.96, 2.05	
	ferric site	ferrous site	ferric site	ferrous site
$\delta$ (mm/s)	0.33	0.70	0.30	0.62
$\Delta E_Q$ (mm/s)	1.09	−3.4	1.0	−3.0
$\eta$	−0.5	−1.7	0	−3
$A_x$ (MHz)	−53.5	8.9	−56	11
$A_y$ (MHz)	−48.1	28.8	−49	27
$A_z$ (MHz)	−44.6	30.2	−42	33

<sup>a</sup>The  $[2\text{Fe-2S}]$  cluster of *A. aeolicus* Fd1 is ligated by four cysteines. Data from ref 18.



The dithionite-reduced protein contains a mononuclear high-spin  $\text{Fe}^{2+}$  contaminant accounting for 8% of the total Fe present. In small applied fields, this contaminant exhibits a doublet with a  $\Delta E_Q$  of 3.35 mm/s and a  $\delta$  of 0.70 mm/s, indicated above the spectrum in Figure 2A. The isomer shift indicates a tetrahedral  $\text{Fe}^{2+}(\text{S})_3\text{X}$  ( $\text{X} = \text{S}, \text{O}, \text{or N}$ ) site. We suspect that the contaminant represents  $[\text{2Fe-2S}]$  sites that lost one iron during the incubation with dithionite.

The fits in Figure 2 reveal that the A tensors of the ferric and ferrous sites have opposite signs, in accord with the standard spin coupling scheme used for  $[\text{2Fe-2S}]^+$  clusters, which predicts  $A(\text{Fe}^{3+}) = (7/3)a(\text{Fe}^{3+})$  and  $A(\text{Fe}^{2+}) = (-4/3)a(\text{Fe}^{3+})$ , where the lowercase quantities refer to the local A tensors of the uncoupled sites. The isomer shift of the ferric site of the  $[\text{2Fe-2S}]^+$  cluster ( $\delta = 0.33$  mm/s) coincides, within experimental error, with the  $\delta(2)$  value of the oxidized cluster for the non-nested assignment. This observation, however, does not imply that the non-nested assignment for the oxidized,  $[\text{2Fe-2S}]^{2+}$  cluster is correct, as the ferric sites of  $[\text{2Fe-2S}]^+$  clusters typically acquire some electron density by valence delocalization (double exchange) from the ferrous site. In fact, all ferric sites of reduced  $[\text{2Fe-2S}]$  clusters have  $\delta$  values that are larger than those observed in the oxidized state. For this reason, we prefer the nested assignment of the two doublets of the oxidized protein. In Table 1, we compare the hyperfine parameters of the reduced IscR protein with those reported for *Aquifex aeolicus* Fd1; for more detailed information, see Table 1 of ref 18. In rough terms, the  $[\text{2Fe-2S}]$  ferredoxins are divided into two classes on the basis of the orientation of the EFG of the ferrous site. For plant-type ferredoxins (e.g., the ferredoxins from spinach and parsley), the largest component of the EFG is negative and along  $z$ , reflecting a  $\beta$  electron in the  $3d_{z^2}$  orbital. In contrast, the largest EFG component of reduced IscR, like that of putidaredoxin, adrenodoxin, and *A. aeolicus* Fd1, is positive ( $\eta < -1$ ) and along  $x$ . Analysis of the electronic structure of the reduced IscR protein is beyond the scope of this study, but we wish to comment briefly on the  $\delta$  value of the ferrous site. The isomer shift of  $\text{Fe}^{2+}$  sites depends on the nature of the coordinated ligands:  $\delta(\text{S}) < \delta(\text{N}) < \delta(\text{O})$ . The isomer shifts of seven well-studied proteins with cysteinyl coordination listed by Meyer et al.<sup>18</sup> range from 0.62 to 0.67 mm/s, with a  $\delta_{\text{ave}}$  of 0.65 mm/s. The ferrous site of Rieske proteins has a  $\delta_{\text{ave}}$  of 0.73 mm/s, reflecting coordination by nitrogens of two histidines. The  $\delta$  value of 0.70 mm/s of IscR is thus more consistent with His-Cys coordination. Moreover, we would expect that the His-coordinated site of IscR has the higher potential and is thus destined to be the reduced site in  $[\text{2Fe-2S}]^+-\text{IscR}$ , as is indeed the case.

**Mössbauer Spectra of Whole Cells.** Figure 3 shows 4.2 K Mössbauer spectra of whole *E. coli* cells. The spectrum in Figure 3A was obtained from cells lacking overexpressed IscR. Roughly 40% of the iron in this sample belongs to a collection of high-spin  $\text{Fe}^{2+}$  species with a  $\Delta E_Q$  of  $\sim 3.0$  mm/s and a  $\delta$  of  $\sim 1.3$  mm/s, outlined by the solid line. Most likely, these species represent octahedral  $\text{Fe}^{2+}$  sites with O and N coordination, as they lack features associated with iron–sulfur clusters or mononuclear  $\text{FeS}_4$  sites. The central feature mostly represents high-spin  $\text{Fe}^{3+}$ , presumably belonging to aggregated iron. Aggregated ferric iron is indicated by broad magnetic features seen in a 5.0 T spectrum (not shown). The spectrum in Figure 3B was obtained from cells overexpressing wild-type IscR. The low-energy feature is readily recognized as belonging to an  $S = 1/2$   $[\text{2Fe-2S}]^+$  cluster, as observed with the purified protein. By

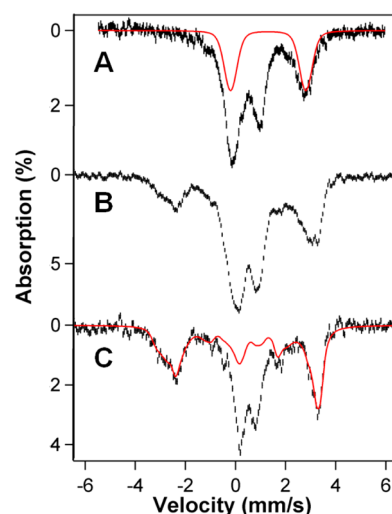


**Figure 3.** Mössbauer spectra of whole cells recorded at 4.2 K in parallel applied fields at 45 mT. (A) Spectrum of whole *E. coli* cells without overexpression of IscR. The red line outlines the contribution of a collection of high-spin  $\text{Fe}^{2+}$  species. (B) Spectrum of whole cells overexpressing wild-type IscR. (C) Spectrum obtained by subtracting spectrum A from spectrum B, assuming that it represents 50% of the Fe in the sample. The procedure gives a good view of the features of the IscR cluster. The red line is the spectral simulation (representing 32% of the Fe) from Figure 2 A (without the 8% contaminant).

subtracting from the spectrum in Figure 3B the spectrum in Figure 3A and assuming that it represents 50% of the total Fe in the cells overexpressing IscR, we obtained the spectrum of Figure 3C; the choice of 50% yields a spectrum whose outer features match those of  $[\text{2Fe-2S}]^+-\text{IscR}$ . The red solid line is the theoretical curve for the purified protein (from Figure 2A), and it represents 32% of the Fe in the sample used to obtain the spectrum in Figure 3B. We do not know which species are contained in the central feature of Figure 3C that is not covered by the red line. We have considered whether it contains contributions from Fe–S clusters. First, if the sample used to obtain Figure 3B contained an oxidized IscR  $[\text{2Fe-2S}]^{2+}$  cluster (there is no direct evidence), it could not represent more than 8% of the Fe. Second, we have no direct evidence of the presence of a  $[\text{4Fe-4S}]^{2+}$  cluster; however, a spectrum recorded at 5.0 T (not shown), in which the absorption of much of the “aggregated” ferric iron is shifted to larger velocities, could accommodate a  $[\text{4Fe-4S}]^{2+}$  cluster (but representing at most 10% of the total Fe) with a  $\Delta E_Q$  of 1 mm/s and a “aggregated” ferric iron is shifted to larger velocities, could of 0.45 mm/s. Thus, in cells containing overexpressed IscR, there are at least 6 times as many  $[\text{2Fe-2S}]^+-\text{IscR}$  clusters as  $[\text{4Fe-4S}]^{2+}-\text{IscR}$  clusters. Even if 10% of the Fe in the sample used to obtain Figure 3B did indeed belong to a  $[\text{4Fe-4S}]^{2+}$  cluster, such a cluster could also belong to proteins other than IscR. Taken together, our data suggest that IscR ligates a  $[\text{2Fe-2S}]$  cluster in vivo and that this cluster is observed predominantly in the reduced state.

**Resonance Raman Data Indicate Partial Non-Cysteiny Ligation of the Cluster to IscR.** Anaerobically isolated  $[\text{2Fe-2S}]-\text{IscR}$  was also characterized by resonance Raman spectroscopy to investigate the cluster ligation scheme. In particular, resonance Raman spectra in the Fe–S stretching region ( $200\text{--}450\text{ cm}^{-1}$ ) of Fe–S cluster-containing proteins can report on the ligation of the cluster.<sup>19–22</sup> Therefore, the resonance Raman spectrum of  $[\text{2Fe-2S}]-\text{IscR}$  isolated under

anaerobic conditions was collected using 488 nm excitation (Figure 4).

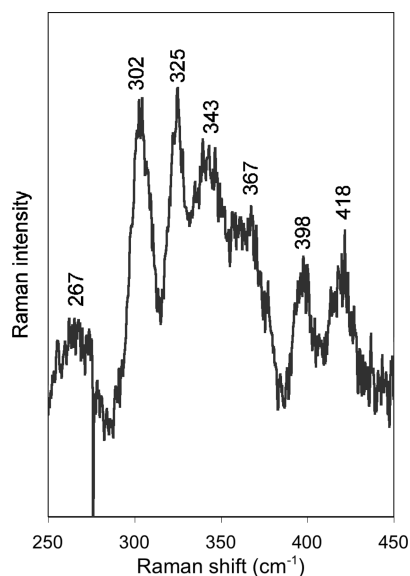


**Figure 4.** 77 K resonance Raman spectrum of anaerobically isolated IscR (47% occupancy, ~3 mM), obtained with laser excitation at 488 nm and a power of 100 mW at the sample (resolution of ~6 cm<sup>-1</sup>). The average of nine scans is presented here, and the contributions from ice lattice vibrations were removed by subtracting a properly scaled spectrum of the buffer obtained under identical conditions.

The spectrum of IscR is not consistent with (Cys)<sub>4</sub> ligation based on a comparison with spectra of well-characterized [2Fe-2S] ferredoxins.<sup>23,24</sup> The b<sub>3u</sub><sup>t</sup> mode with predominant Fe–S<sup>t</sup> stretching character occurs in the range of 281–292 cm<sup>-1</sup> (one broad band) in spectra of these ferredoxins with (Cys)<sub>4</sub> ligation. This band is upshifted in the spectra of proteins that ligate [2Fe-2S] clusters via three cysteines and either one serine or one aspartate.<sup>20–22</sup> For example, the b<sub>3u</sub><sup>t</sup> mode is upshifted from 292 to 302 cm<sup>-1</sup> upon substitution of a coordinating cysteine ligand with serine in the [2Fe-2S]-ferredoxin of *Clostridium pasteurianum*.<sup>21</sup> Therefore, the presence of a band at 302 cm<sup>-1</sup> in the spectrum of IscR could suggest (Cys)<sub>3</sub>(O)<sub>1</sub> ligation of the cluster.

However, the presence of a band at 267 cm<sup>-1</sup> in conjunction with a band at 302 cm<sup>-1</sup> in the spectrum of IscR suggests that the unidentified fourth ligand could be a histidine. The spectra of Rieske-type [2Fe-2S] clusters with (Cys)<sub>2</sub>(His)<sub>2</sub> ligation display two peaks in this low-frequency region that are sensitive to perturbations to the Fe–His bonding interactions.<sup>25</sup> For example, the spectrum of the archaeal Rieske-type ferredoxin of *Sulfolobus solfataricus* exhibits peaks at 260 and 310 cm<sup>-1</sup> that are downshifted to 258 and 304 cm<sup>-1</sup>, respectively, upon substitution of one cluster-ligating histidine with cysteine to create (Cys)<sub>3</sub>(His)<sub>1</sub> ligation.<sup>26</sup> Similar to the spectra of Rieske clusters, the resonance Raman spectra of both the (Cys)<sub>3</sub>(His)<sub>1</sub>-coordinated [2Fe-2S]-Fra2–Grx3 complex (275 and 300 cm<sup>-1</sup>)<sup>10</sup> and structurally characterized (Cys)<sub>3</sub>(His)<sub>1</sub>-coordinated [2Fe-2S]-mitoNEET (~265 and ~295 cm<sup>-1</sup>)<sup>27</sup> exhibit two bands in the 250–320 cm<sup>-1</sup> region that suggest partial histidyl ligation. In contrast, the substitution of the histidine ligand of mitoNEET with cysteine, creating (Cys)<sub>4</sub> ligation, results in the appearance of only a single band at ~280

cm<sup>-1</sup> in the resonance Raman spectrum, consistent with the spectra of other [2Fe-2S] clusters ligated by four cysteines.<sup>10,27</sup>

Therefore, the resonance Raman spectrum of [2Fe-2S]-IscR is consistent with coordination of the [2Fe-2S] cluster by three cysteines and one other ligand that ligates the cluster via an O atom or a N atom. The resonance Raman spectrum of D<sub>2</sub>O-exchanged IscR was nearly identical to that of the protein before exchange (data not shown), ruling out the possibility of a cluster-ligating bridging water/hydroxide molecule. Therefore, mutagenesis studies were performed to identify the amino acid side chain necessary for cluster ligation.

#### His107 Is Essential for Ligation of the Cluster to IscR.

Because collectively the Mössbauer and resonance Raman data suggested that the [2Fe-2S] cluster is coordinated via an O atom or a N atom, we substituted with alanine mostly conserved amino acids that could potentially ligate the cluster via an O atom or a N atom. The targeted amino acids included several highly conserved residues near the cysteine-rich region of IscR (Tyr65, Asp84, Glu85, Thr106, His107, and Trp110), the Glu43 residue in the DNA binding domain that has been proposed to be the fourth ligand to the IscR cluster in *Acidithiobacillus ferrooxidans*,<sup>28</sup> and the other histidines of IscR, His143 and His145. If any of these residues acted as the fourth cluster ligand, we would expect that an alanine substitution at that position would remove an O bond or a N bond to the cluster. Hence, such a substitution should result in a protein variant that most likely would lack an Fe–S cluster upon isolation and would be defective in repressing the *iscR* promoter.

IscR variants were tested for their ability to repress the *iscR* promoter under anaerobic growth conditions as an indication of the ability of the variants to ligate an Fe–S cluster in vivo. In contrast to the strain expressing WT IscR, P<sub>iscR</sub>-*lacZ* was not repressed under anaerobic growth conditions in a strain containing IscR with alanine substitutions of all three cluster-coordinating cysteines (the triple mutant, IscR-C92A/C98A/C104A), consistent with cluster ligation by IscR being required for repression of the *iscR* promoter. Of the other variants tested, only IscR-H107A displayed the same defective phenotype as IscR-C92A/C98A/C104A (Figure 5A and data not shown). Importantly, the lack of repression by IscR-C92A/C98A/C104A and IscR-H107A was not due to any substantial decrease in protein levels compared to WT levels, as determined by Western blot analysis (data not shown). The lack of activity of IscR-H107A in vivo was correlated with the lack of the Fe–S cluster in vitro, because isolation of IscR-H107A under anaerobic conditions yielded apoprotein (Figure 5B). In contrast, WT IscR, IscR-E43A, and the double mutant IscR-H143A/H145A, for example, were occupied with cluster when isolated under the same anaerobic conditions. These results suggest that His107 is important for binding of the cluster to IscR.

The effect of substituting His107 with cysteine, to potentially create a (Cys)<sub>4</sub>-ligated cluster, was also tested. Partial repression of P<sub>iscR</sub>-*lacZ* was observed when the strain containing IscR-H107C was tested under anaerobic growth conditions, suggesting some Fe–S cluster coordination in vivo (Figure 5A). Despite some activity in vivo, there was no detectable [2Fe-2S] cluster in anaerobically isolated IscR-H107C (Figure 5B). Because activity in vivo reflects both synthesis and turnover, a mutant with reduced cluster stability can still demonstrate activity, if the rate of synthesis is greater than the rate of cluster turnover. However, isolated protein only reflects the lability of

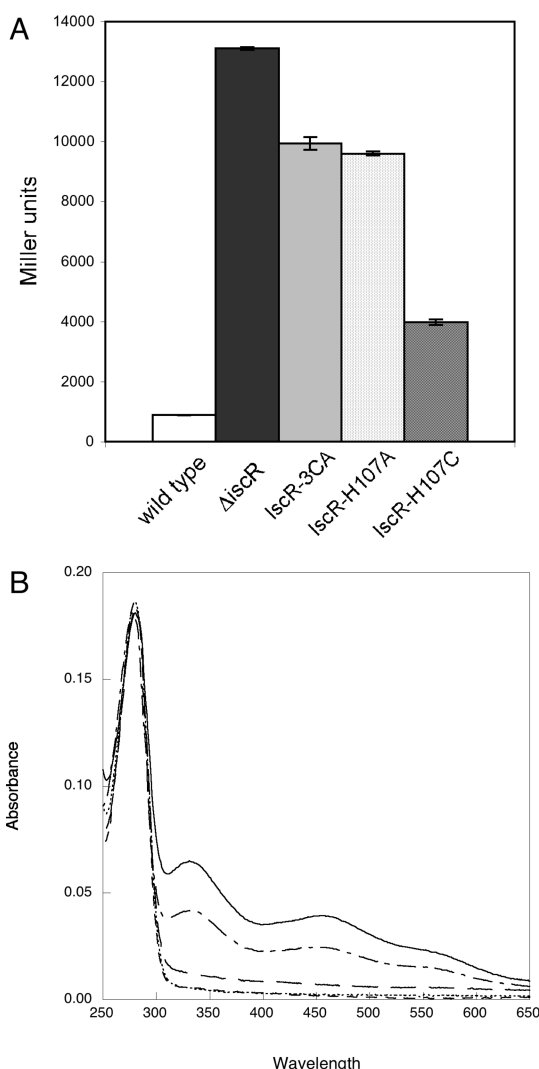


**Figure 5.** (A) Expression levels of the *iscR* promoter fused to *lacZ* were determined in strains containing wild-type IscR (white bar),  $\Delta$ *iscR* (black bar), IscR-C92A/C98A/C104A (IscR-3CA, gray bar), IscR-H107A (light patterned bar), or IscR-H107C (dark patterned bar). Strains were grown under anaerobic conditions in MOPS minimal medium containing 0.2% glucose and were assayed for  $\beta$ -galactosidase activity per OD<sub>600</sub> (Miller units). (B) Optical spectra of IscR variants. The spectra of wild-type IscR (—), IscR-E43A (---), IscR-C92A/C98A/C104A (----), IscR-H107A (----), and IscR-H107C (.....) were obtained under anaerobic conditions in 10 mM HEPES (pH 7.4) with 200 mM KCl at room temperature (10  $\mu$ M protein). All variants were isolated under anaerobic conditions as described in Methods.

the cluster. Thus, the cluster of the variant protein is not as stable as the cluster present in WT IscR. Cluster instability has previously been observed in the Fra2–Grx3 complex upon substitution of the histidine cluster ligand with cysteine, likely because of lengthening of the Fe–Fe distance and the original Fe–S bond distances.<sup>11</sup> However, the observation that cysteine can partially substitute for histidine in IscR is consistent with the imidazole ring of His107 being structurally poised to act as a direct cluster ligand.

**<sup>15</sup>N NMR Supports the Hypothesis That His107 Is a Cluster Ligand in [2Fe-2S]-IscR.** <sup>15</sup>N NMR spectra were recorded with rapid recycling times for three samples of the reduced holoprotein at pH 6.4 and 298 K: [U-<sup>15</sup>N]IscR(WT)

(Figure 6A), [U-<sup>15</sup>N]IscR(H143A/H145A) (Figure 6B), and [U-<sup>15</sup>N,NA-His]IscR(WT) (Figure 6C). Comparison of these

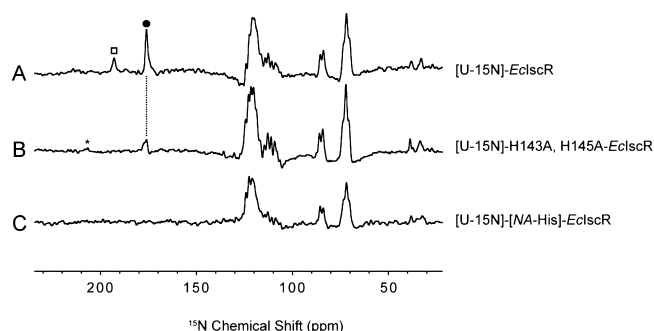


**Figure 6.** <sup>15</sup>N NMR spectra of ~2 mM reduced IscR samples recorded at pH 6.4 and 298 K under rapid pulsing conditions. (A) [U-<sup>15</sup>N]IscR(WT) produced from cells grown on <sup>15</sup>NH<sub>4</sub>Cl as the sole nitrogen source. (B) [U-<sup>15</sup>N]IscR(H143A/H145A) produced from cells grown on <sup>15</sup>NH<sub>4</sub>Cl as the sole nitrogen source. (C) [U-<sup>15</sup>N]IscR(WT) produced from cells grown on <sup>15</sup>NH<sub>4</sub>Cl in the presence of unlabeled L-histidine. Together, these spectra show that the indicated signals (□ and ●) in panel A arise from histidine residues and that the signal labeled with a filled circle is from His107, the one His residue not removed by substitution in the sample whose spectrum is shown in panel B. The peak labeled with an empty square appeared in other spectra of [U-<sup>15</sup>N]IscR(H143A/H145A) (not shown). The peak labeled with an asterisk is from <sup>14</sup>N and <sup>15</sup>N in nitrogen gas in air.

spectra identified two <sup>15</sup>N peaks arising from rapidly relaxing histidine residues and further identified one of these signals as arising from His107. Because of the lower protein concentration of [U-<sup>15</sup>N]IscR(H143A/H145A), the sensitivity was insufficient to resolve the second signal in the spectrum of this sample (Figure 6B); however, the second signal was observed in spectra collected at higher temperatures. These results allowed us to assign the two <sup>15</sup>N peaks to His107. Comparison of <sup>15</sup>N NMR spectra of [U-<sup>15</sup>N]IscR(WT) recorded at 298 K (Figure 7A) and 288 K (Figure 7B) showed that the two peaks assigned to His107 shifted to higher frequencies at higher temperatures. Comparison of <sup>15</sup>N NMR spectra of [U-<sup>15</sup>N]-IscR(WT) recorded at two different delays between acquisition pulses (1.0 s and 5.0 ms) confirmed that the signals assigned to His107 relax rapidly, as expected for an Fe–S cluster ligand. We investigated the pH dependence of the two <sup>15</sup>N signals assigned to His107 and found that the signal at the higher frequency exhibited a larger titration shift than that at the lower frequency (Figure 8A). Each signal shifted continuously with pH, indicating rapid proton exchange between the two protonation states. Both signals were observed to sharpen in the protonated state at low pH.

**The Cluster Oxidation State Does Not Influence the DNA Binding Properties of Holo-IscR.** As discerned from Mössbauer spectroscopy, the cluster of IscR is primarily in the reduced form *in vivo* and is partially oxidized upon anaerobic isolation of the protein. In addition, previous studies of the [2Fe-2S] cluster of anaerobically isolated IscR illustrate that the cluster can be oxidized by O<sub>2</sub> and reversibly reduced without significant decomposition.<sup>2</sup> Therefore, by comparing the affinity of O<sub>2</sub>-exposed IscR for dsDNA containing the *iscR* site in the absence and presence of dithionite, we can explore whether the oxidation state of the cluster affects the ability of IscR to bind to the *iscR* promoter. *In vitro* DNA binding assays



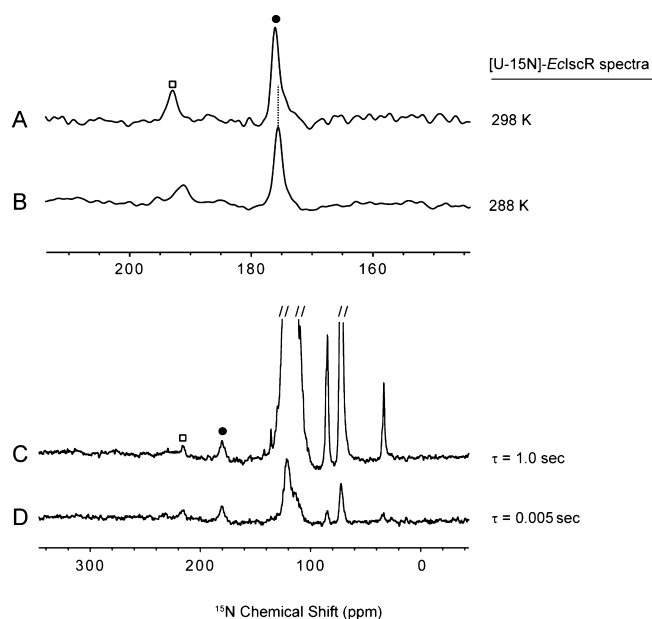


**Figure 7.** Evidence from  $^{15}\text{N}$  NMR spectra that the labeled signals ( $\square$  and  $\bullet$ ) of reduced  $[\text{U}-^{15}\text{N}]\text{IscR}(\text{WT})$  arise from nuclei affected by electron–nuclear (hyperfine) interactions. (A and B) Chemical shifts of the labeled peaks exhibit anti-Curie shifts as a function of temperature as expected for an Fe–S cluster ligand (delay value of 5.0 ms). (C and D) Spectra recorded as two different delay values (1.0 s and 5.0 ms) between the data collection pulses suggest that the labeled peaks correspond to rapidly relaxing nuclei, as expected for a cluster ligand.

illustrate that air-oxidized IscR (containing predominantly  $[\text{2Fe-2S}]^{2+}$ ) bound to dsDNA containing the *iscR* binding site with an affinity similar to that of dithionite-reduced IscR containing predominantly  $[\text{2Fe-2S}]^+$  (Figure 9). Therefore, oxidation of the cluster of IscR from  $[\text{2Fe-2S}]^+$  to  $[\text{2Fe-2S}]^{2+}$  does not appear to affect the DNA binding properties.

## DISCUSSION

IscR is a global regulator involved in a homeostatic mechanism controlling Fe–S cluster biogenesis and is proposed to act as a sensor of the cellular demands for Fe–S cluster biogenesis. The mechanism by which IscR senses the demand has not yet been detailed, but we expect that the Fe–S cluster of IscR has some unusual features that are relevant to this function. Indeed, the data presented here suggest that IscR of *E. coli* contains a reduced  $[\text{2Fe-2S}]^+$  cluster in vivo with  $(\text{Cys})_3(\text{His})_1$  ligation, which is a fairly uncommon ligation scheme.

All of the spectroscopic data are consistent with  $(\text{Cys})_3(\text{His})_1$  ligation. The  $^{15}\text{N}$  NMR data were particularly informative in assigning His107 to a likely role in cluster ligation. The intensities of the two signals assigned to His107 decreased upon oxidation of the protein (data not shown), indicating that their chemical shifts are highly dependent on the redox state. The two  $^{15}\text{N}$  signals exhibited rapid relaxation and an anti-Curie temperature dependence (i.e., increasing paramagnetic shifts with decreasing temperature), as expected for a ligand bound to an antiferromagnetically coupled cluster. Both signals exhibited pH titration shifts of the type observed for His imidazole ring nitrogens ( $^{15}\text{N}^{\delta 1}$  and  $^{15}\text{N}^{\epsilon 2}$ ) ligated to a  $[\text{2Fe-2S}]$  cluster in a Rieske protein.<sup>29,30</sup> In Rieske proteins, however,  $^{15}\text{N}$  signals could not be resolved from ring nitrogens ligated to the iron,<sup>29–31</sup> presumably because they were too broad to be

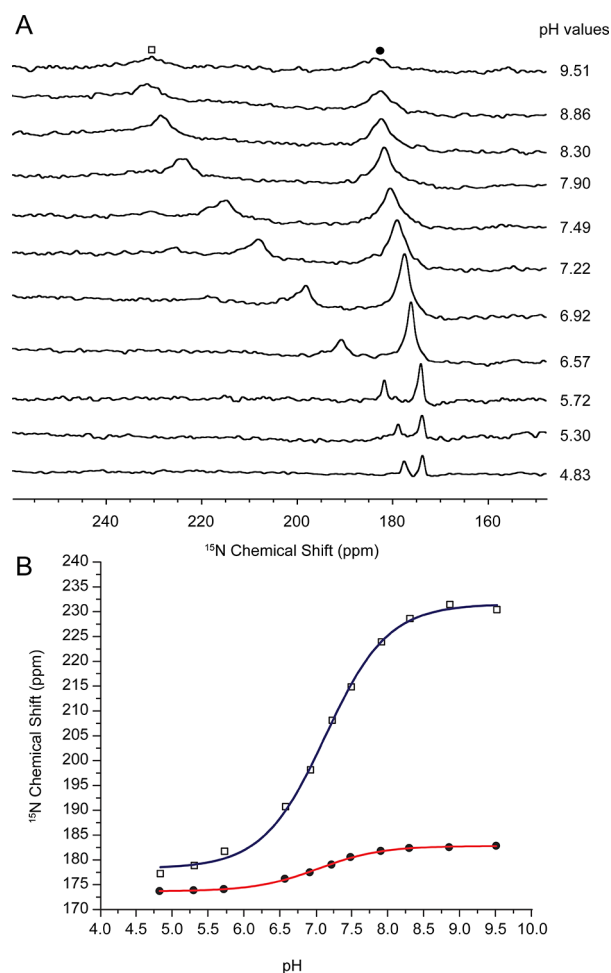


**Figure 8.** (A) Dependence of  $^{15}\text{N}$  NMR spectra of 2 mM reduced  $[\text{U}-^{15}\text{N}]\text{IscR}(\text{WT})$  recorded at 298 K at the pH of the sample. (B) Plot of the pH dependence of the chemical shifts of peak 1 ( $\square$ ) and peak 2 ( $\bullet$ ). The data were fit to theoretical curves, which yielded a  $\text{pK}_{\text{a}1}$  of  $7.12 \pm 0.03$  (blue line) and a  $\text{pK}_{\text{a}2}$  of  $7.04 \pm 0.02$  (red line). The uncertainties are those from curve fitting. We consider these  $\text{pK}_{\text{a}}$  values to be equal within experimental error.

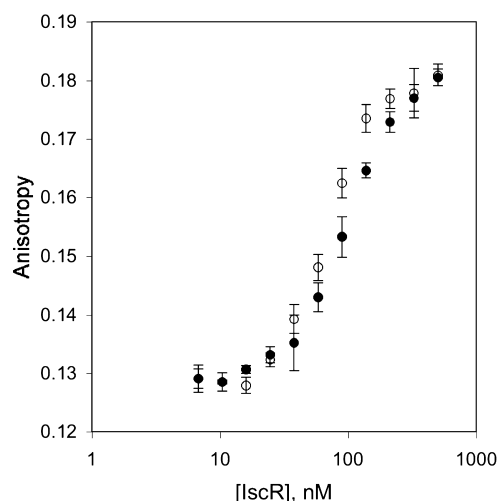


**Figure 9.** In vitro DNA binding assays. As-isolated IscR was exposed to air and then tested for its ability to bind to double-stranded DNA containing the *iscR* binding site in the absence ( $\bullet$ ) or presence ( $\circ$ ) of 10  $\mu\text{M}$  dithionite.

detected. We suspect that the broader peak at a higher frequency (Figures 6–8) corresponds to the nitrogen atom ligated to Fe. The fact that this signal is observed suggests that the degree of unpaired electron spin delocalization onto this atom is lower in a (Cys)<sub>3</sub>(His)<sub>1</sub>-ligated Fe–S protein than in a (Cys)<sub>2</sub>(His)<sub>2</sub>-ligated Rieske protein. The sharpening of the <sup>15</sup>N NMR signals at low pH indicates that the addition of a positively charged proton to the ligand His weakens its interaction with the positively charged cluster.

Interestingly, a number of proteins currently identified as binding a [2Fe-2S] cluster with (Cys)<sub>3</sub>(His)<sub>1</sub> ligation appear to have possible roles as sensors. IscR directly regulates the transcription of the *isc* operon, which encodes the proteins that constitute the primary pathway of Fe–S cluster biogenesis in *E. coli*.<sup>2</sup> Further, the role of IscR has been expanded to include a role as a global regulator that senses and responds to the cellular demand for cluster synthesis and/or repair.<sup>1,5</sup> The yeast proteins Fra2 and Grx3 are involved in sensing the cellular iron status and subsequently transmitting a signal to the transcriptional activators Aft1 and Aft2.<sup>32–34</sup> Although the mechanism has not been elucidated, Aft1/2 activity is inhibited under iron-replete conditions via interactions with the Fra2 and Grx3 proteins that promote the export of Aft1/2 from the nucleus. Lastly, the function of the mitochondrial protein mitoNEET is not as well-defined as those of the proteins discussed here. However, the [2Fe-2S] cluster of mitoNEET, which is not stable in vitro below pH 8,<sup>35</sup> is stabilized by the binding of the thiazolidinedione class of anti-diabetes drugs.<sup>36,37</sup> As this class of drugs is known to enhance oxidative capacity, ligation of an Fe–S cluster to mitoNEET may allow it to act as a sensor of oxidative stress or, perhaps because of the intimate link between the two,<sup>38</sup> the cellular iron status. Whether a sensor function will be assigned to other, yet to be identified, proteins that bind [2Fe-2S] clusters with (Cys)<sub>3</sub>(His)<sub>1</sub> ligation remains to be seen.

It is also of interest to consider the ligation of Fe–S clusters to other transcription factors with sensor functions as we attempt to understand the cluster and protein features that define sensor function. An example of note is the NO sensor NsrR, which is a member of the Rrf2 family of transcription factors that includes IscR. While the three cysteines are conserved between IscR and NsrR, His107 is not conserved.<sup>9</sup> Rather, the residue corresponding to His107 in *E. coli* NsrR is lysine, and preliminary data suggest that *E. coli* IscR-H107K is in the apo form upon anaerobic isolation. Whether the apparent difference in cluster ligands between IscR, a sensor of Fe–S cluster demand, and NsrR, a sensor of NO, is related to their differing sensor functions remains to be seen.

The recognition of an atypical ligation scheme for the [2Fe-2S] cluster of IscR does, however, provide some new insight into investigating possible sensing mechanisms. The feedback model of IscR repression proposes that IscR acquires an Fe–S cluster via the Isc proteins once the cellular demand for Fe–S cluster biogenesis is satisfied,<sup>2</sup> suggesting that the Isc proteins might be able to distinguish between IscR and other apoprotein targets. While the details of target specificity of the Isc proteins remain elusive,<sup>39</sup> the proposed (Cys)<sub>3</sub>(His)<sub>1</sub> ligation scheme of IscR could differentiate it from other apoproteins. Perhaps by making IscR a poor substrate for the Isc proteins via one atypical amino acid ligand, IscR is able to sense the cellular demand for Fe–S cluster biogenesis indirectly by the availability of the Isc machinery to associate with IscR.

The ligation scheme observed for IscR does not appear to confer any unusual sensitivity to O<sub>2</sub> that could make the Fe–S cluster occupancy of IscR sensitive to the general cellular demands for Fe–S cluster biogenesis. In vivo, [2Fe-2S]-IscR regulates the *iscR* promoter and appears to be mostly in the reduced state under anaerobic growth conditions. However, changes in the cluster oxidation state upon exposure to O<sub>2</sub> do not alter the ability of IscR to bind to the *iscR* site in vitro, suggesting that changes in cluster oxidation state may not be relevant to the sensor function of IscR. Therefore, IscR may not directly respond to O<sub>2</sub>, and the functional relevance of the ability of [2Fe-2S]-IscR to be reversibly oxidized and reduced is not clear. However, the data do not preclude the possibility that the proposed (Cys)<sub>3</sub>(His)<sub>1</sub> cluster ligation scheme makes IscR more prone to cluster loss upon prolonged exposure to O<sub>2</sub> or reactive oxygen species, which will be addressed in further studies.

The identification of His107 as a likely cluster ligand in IscR of *E. coli* also has implications for the structure–function relationship of IscR. As IscR function is linked to cluster binding, interactions between the DNA-binding domain and cluster-binding domain are likely essential for IscR function. The proposal that Glu43, a residue in the predicted DNA binding domain, acts as the fourth ligand to the cluster in IscR of *Ab. ferrooxidans*<sup>28</sup> suggested a direct mechanism for the communication of cluster acquisition (or loss) between the two domains. However, on the basis of the recent X-ray crystal structure of *Bacillus subtilis* CymR, a member of the Rrf2 family of transcription factors, Glu43 (Glu44 in CymR) is expected to make direct contacts to the DNA site and thus does not appear to be structurally poised to act as a cluster ligand.<sup>40</sup> Therefore, communication of cluster acquisition (or loss) to the DNA binding domain is more likely to occur via interactions between residues in the cluster-binding region of one monomer and residues in the DNA-binding region of the other monomer of the IscR homodimer, similar to what was observed in the X-ray crystal structure of transcription factor [2Fe-2S]<sup>2+</sup>-SoxR of *E. coli*.<sup>41</sup> The conformational changes that occur upon binding of the cluster to IscR are not yet known.

## AUTHOR INFORMATION

### Corresponding Author

\*Address: 4204C Biochemical Sciences Building, 440 Henry Mall, Madison, WI 53706. E-mail: pj.kiley@wisc.edu. Telephone: (608) 262-6632. Fax: (608) 262-5253.

### Funding

This work was supported by National Institutes of Health Grants F32GM085987 (A.S.F.), GM45844 (P.J.K.), R01GM58667 (J.L.M.), and P41RR02301 (J.L.M.), and the National Science Foundation Grant MCB 0424494 (E.M.).

### Notes

The authors declare no competing financial interest.

## REFERENCES

- (1) Giel, J. L., Rodionov, D., Liu, M. Z., Blattner, F. R., and Kiley, P. J. (2006) IscR-dependent gene expression links iron-sulphur cluster assembly to the control of O<sub>2</sub>-regulated genes in *Escherichia coli*. *Mol. Microbiol.* 60, 1058–1075.
- (2) Schwartz, C. J., Giel, J. L., Patschkowski, T., Luther, C., Ruzicka, F. J., Beinert, H., and Kiley, P. J. (2001) IscR, an Fe-S cluster-containing transcription factor, represses expression of *Escherichia coli* genes encoding Fe-S cluster assembly proteins. *Proc. Natl. Acad. Sci. U.S.A.* 98, 14895–14900.



- (3) Frazzon, J., and Dean, D. R. (2001) Feedback regulation of iron-sulfur cluster biosynthesis. *Proc. Natl. Acad. Sci. U.S.A.* 98, 14751–14753.
- (4) Yeo, W. S., Lee, J. H., Lee, K. C., and Roe, J. H. (2006) IscR acts as an activator in response to oxidative stress for the *suf* operon encoding Fe-S assembly proteins. *Mol. Microbiol.* 61, 206–218.
- (5) Nesbit, A. D., Giel, J. L., Rose, J. C., and Kiley, P. J. (2009) Sequence-specific binding to a subset of IscR-regulated promoters does not require IscR Fe-S cluster ligation. *J. Mol. Biol.* 387, 28–41.
- (6) Guigliarelli, B., and Bertrand, P. (1999) Application of EPR spectroscopy to the structural and functional study of iron-sulfur proteins. *Adv. Inorg. Chem.* 47, 421–497.
- (7) Orio, M., and Mouesca, J. M. (2008) Variation of average *g* values and effective exchange coupling constants among [2Fe-2S] clusters: A density functional theory study of the impact of localization (trapping forces) versus delocalization (double-exchange) as competing factors. *Inorg. Chem.* 47, 5394–5416.
- (8) Finn, R. D., Mistry, J., Tate, J., Coghill, P., Heger, A., Pollington, J. E., Gavin, O. L., Gunasekaran, P., Ceric, G., Forslund, K., Holm, L., Sonnhammer, E. L. L., Eddy, S. R., and Bateman, A. (2010) The Pfam protein families database. *Nucleic Acids Res.* 38, D211–D222.
- (9) Tucker, N. P., Le Brun, N. E., Dixon, R., and Hutchings, M. I. (2010) There's NO stopping NsrR, a global regulator of the bacterial NO stress response. *Trends Microbiol.* 18, 149–156.
- (10) Li, H. R., Mapolelo, D. T., Dingra, N. N., Naik, S. G., Lees, N. S., Hoffman, B. M., Riggs-Gelasco, P. J., Huynh, B. H., Johnson, M. K., and Outten, C. E. (2009) The yeast iron regulatory proteins Grx3/4 and Fra2 form heterodimeric complexes containing a [2Fe-2S] cluster with cysteinyl and histidyl ligation. *Biochemistry* 48, 9569–9581.
- (11) Li, H. R., Mapolelo, D. T., Dingra, N. N., Keller, G., Riggs-Gelasco, P. J., Winge, D. R., Johnson, M. K., and Outten, C. E. (2011) Histidine-103 in Fra2 is an iron-sulfur cluster ligand in the [2Fe-2S] Fra2-Grx3 complex and is required for *in vivo* iron signaling in yeast. *J. Biol. Chem.* 286, 867–876.
- (12) Yan, A. X., and Kiley, P. J. (2009) Techniques to isolate O<sub>2</sub>-sensitive proteins: [4Fe-4S]-FNR as an example. *Methods Enzymol.* 463, 787–805.
- (13) Khoroshilova, N., Popescu, C., Munck, E., Beinert, H., and Kiley, P. J. (1997) Iron-sulfur cluster disassembly in the FNR protein of *Escherichia coli* by O<sub>2</sub>: 4Fe-4S to 2Fe-2S conversion with loss of biological activity. *Proc. Natl. Acad. Sci. U.S.A.* 94, 6087–6092.
- (14) Popescu, C. V., Bates, D. M., Beinert, H., Münck, E., and Kiley, P. J. (1998) Mössbauer spectroscopy as a tool for the study of activation/inactivation of the transcription regulator FNR in whole cells of *Escherichia coli*. *Proc. Natl. Acad. Sci. U.S.A.* 95, 13431–13435.
- (15) Sutton, V. R., Stubna, A., Patschkowski, T., Münck, E., Beinert, H., and Kiley, P. J. (2004) Superoxide destroys the [2Fe-2S]<sup>2+</sup> cluster of FNR from *Escherichia coli*. *Biochemistry* 43, 791–798.
- (16) Miller, J. H. (1972) *Experiments in Molecular Genetics*, Cold Spring Harbor Laboratory Press, Plainview, NY.
- (17) Münck, E. (1978) Mössbauer spectroscopy of proteins: Electron carriers. *Methods Enzymol.* 54, 346–379.
- (18) Meyer, J., Clay, M. D., Johnson, M. K., Stubna, A., Munck, E., Higgins, C., and Wittung-Stafshede, P. (2002) A hyperthermophilic plant-type 2Fe-2S ferredoxin from *Aquifex aeolicus* is stabilized by a disulfide bond. *Biochemistry* 41, 3096–3108.
- (19) Kuila, D., Schoonover, J. R., Dyer, R. B., Batie, C. J., Ballou, D. P., Fee, J. A., and Woodruff, W. H. (1992) Resonance Raman studies of Rieske-type proteins. *Biochim. Biophys. Acta* 1140, 175–183.
- (20) Crouse, B. R., Sellers, V. M., Finnegan, M. G., Dailey, H. A., and Johnson, M. K. (1996) Site-directed mutagenesis and spectroscopic characterization of human ferrochelatase: Identification of residues coordinating the [2Fe-2S] cluster. *Biochemistry* 35, 16222–16229.
- (21) Meyer, J., Fujinaga, J., Gaillard, J., and Lutz, M. (1994) Mutated forms of the [2Fe-2S] ferredoxin from *Clostridium pasteurianum* with noncysteine ligands to the iron-sulfur cluster. *Biochemistry* 33, 13642–13650.
- (22) Duin, E. C., Lafferty, M. E., Crouse, B. R., Allen, R. M., Sanyal, I., Flint, D. H., and Johnson, M. K. (1997) [2Fe-2S] to [4Fe-4S] cluster conversion in *Escherichia coli* biotin synthase. *Biochemistry* 36, 11811–11820.
- (23) Han, S., Czernuszewicz, R. S., Kimura, T., Adams, M. W. W., and Spiro, T. G. (1989) Fe<sub>2</sub>S<sub>2</sub> protein resonance Raman-spectra revisited: Structural variations among adrenodoxin, ferredoxin, and red paramagnetic protein. *J. Am. Chem. Soc.* 111, 3505–3511.
- (24) Fu, W. G., Drozdowski, P. M., Davies, M. D., Sligar, S. G., and Johnson, M. K. (1992) Resonance Raman and magnetic circular dichroism studies of reduced [2Fe-2S] proteins. *J. Biol. Chem.* 267, 15502–15510.
- (25) Rotsaert, F. A. J., Pikus, J. D., Fox, B. G., Markley, J. L., and Sanders-Loehr, J. (2003) N-isotope effects on the Raman spectra of Fe<sub>2</sub>S<sub>2</sub> ferredoxin and Rieske ferredoxin: Evidence for structural rigidity of metal sites. *J. Biol. Inorg. Chem.* 8, 318–326.
- (26) Kounosu, A., Li, Z. R., Cosper, N. J., Shokes, J. E., Scott, R. A., Imai, T., Urushiyama, A., and Iwasaki, T. (2004) Engineering a three-cysteine, one-histidine ligand environment into a new hyperthermophilic archaeal Rieske-type [2Fe-2S] ferredoxin from *Sulfolobus solfataricus*. *J. Biol. Chem.* 279, 12519–12528.
- (27) Tirrell, T. F., Paddock, M. L., Conlan, A. R., Smoll, E. J., Nechushtai, R., Jennings, P. A., and Kim, J. E. (2009) Resonance Raman studies of the (His)(Cys)<sub>3</sub> 2Fe-2S Cluster of mitoNEET: Comparison to the (Cys)<sub>4</sub> mutant and implications of the effects of pH on the labile metal center. *Biochemistry* 48, 4747–4752.
- (28) Zeng, J., Zhang, X. J., Wang, Y. P., Ai, C. B., Liu, Q., and Qiu, G. Z. (2008) Glu43 is an essential residue for coordinating the [Fe<sub>2</sub>S<sub>2</sub>] cluster of IscR from *Acidithiobacillus ferrooxidans*. *FEBS Lett.* 582, 3889–3892.
- (29) Lin, L.-J., Chen, Y., Fee, J. A., Song, J. K., Westler, W. M., and Markley, J. L. (2006) Rieske protein from *Thermus thermophilus*: <sup>15</sup>N NMR titration study demonstrates the role of iron-ligated histidines in the pH dependence of the reduction potential. *J. Am. Chem. Soc.* 128, 10672–10673.
- (30) Hsueh, K.-L., Westler, W. M., and Markley, J. L. (2010) NMR investigation of the Rieske protein from *Thermus thermophilus* support a coupled proton and electron transfer mechanism. *J. Am. Chem. Soc.* 132, 7908–7918.
- (31) Xia, B., Pikus, J. D., Xia, W. D., McClay, K., Steffan, R. J., Chae, Y. K., Westler, W. M., Markley, J. L., and Fox, B. G. (1999) Detection and classification of hyperfine-shifted <sup>1</sup>H, <sup>2</sup>H, and <sup>15</sup>N resonances of the Rieske ferredoxin component of toluene 4-monooxygenase. *Biochemistry* 38, 727–739.
- (32) Kumanovics, A., Chen, O. S., Li, L. T., Bagley, D., Adkins, E. M., Lin, H. L., Dingra, N. N., Outten, C. E., Keller, G., Winge, D., Ward, D. M., and Kaplan, J. (2008) Identification of FRA1 and FRA2 as genes involved in regulating the yeast iron regulon in response to decreased mitochondrial iron-sulfur cluster synthesis. *J. Biol. Chem.* 283, 10276–10286.
- (33) Ojeda, L., Keller, G., Muhlenhoff, U., Rutherford, J. C., Lill, R., and Winge, D. R. (2006) Role of glutaredoxin-3 and glutaredoxin-4 in the iron regulation of the Aft1 transcriptional activator in *Saccharomyces cerevisiae*. *J. Biol. Chem.* 281, 17661–17669.
- (34) Pujol-Carrion, N., Belli, G., Herrero, E., Nogues, A., and de la Torre-Ruiz, M. A. (2006) Glutaredoxins Grx3 and Grx4 regulate nuclear localisation of Aft1 and the oxidative stress response in *Saccharomyces cerevisiae*. *J. Cell Sci.* 119, 4554–4564.
- (35) Wiley, S. E., Paddock, M. L., Abresch, E. C., Gross, L., van der Geer, P., Nechushtai, R., Murphy, A. N., Jennings, P. A., and Dixon, J. E. (2007) The outer mitochondrial membrane protein mitoNEET contains a novel redox-active 2Fe-2S cluster. *J. Biol. Chem.* 282, 23745–23749.
- (36) Paddock, M. L., Wiley, S. E., Axelrod, H. L., Cohen, A. E., Roy, M., Abresch, E. C., Capraro, D., Murphy, A. N., Nechushtai, R., Dixon, J. E., and Jennings, P. A. (2007) MitoNEET is a uniquely folded 2Fe-2S outer mitochondrial membrane protein stabilized by pioglitazone. *Proc. Natl. Acad. Sci. U.S.A.* 104, 14342–14347.
- (37) Bak, D. W., Zuris, J. A., Paddock, M. L., Jennings, P. A., and Elliott, S. J. (2009) Redox characterization of the FeS protein

mitoNEET and impact of thiazolidinedione drug binding. *Biochemistry* 48, 10193–10195.

(38) Imlay, J. A. (2008) Cellular defenses against superoxide and hydrogen peroxide. *Annu. Rev. Biochem.* 77, 755–776.

(39) Ayala-Castro, C., Saini, A., and Outten, F. W. (2008) Fe-S cluster assembly pathways in bacteria. *Microbiol. Mol. Biol. Rev.* 72, 110–125.

(40) Shepard, W., Soutourina, O., Courtois, E., England, P., Haouz, A., and Martin-Verstraete, I. (2011) Insights into the Rrf2 repressor family: The structure of CymR, the global cysteine regulator of *Bacillus subtilis*. *FEBS J.* 278, 2689–2701.

(41) Watanabe, S., Kita, A., Kobayashi, K., and Miki, K. (2008) Crystal structure of the [2Fe-2S] oxidative-stress sensor SoxR bound to DNA. *Proc. Natl. Acad. Sci. U.S.A.* 105, 4121–4126.